ABSTRACT

Title of Dissertation: FINDING OPTIMAL ORBITS OF CHAOTIC SYSTEMS

Angela Elyse Grant, Doctor of Philosophy, 2005

Dissertation directed by: Professor Brian R. Hunt
Department of Mathematics

Chaotic dynamical systems can exhibit a wide variety of motions, including periodic orbits of arbitrarily large period. We consider the question of which motion is optimal, in the sense that it maximizes the average over time of some given scalar "performance function." Past work indicates that optimal motions tend to be periodic orbits with low period, but does not describe, beyond a brute force approach, how to determine which orbit is optimal in a particular scenario. For one-dimensional expanding maps and higher dimensional hyperbolic systems, we have found constructive methods for calculating the optimal average and corresponding periodic orbit, and by carrying them out on a computer have found them to work quite well in practice.

FINDING OPTIMAL ORBITS OF CHAOTIC SYSTEMS

by

Angela Elyse Grant

Dissertation submitted to the Faculty of the Graduate School of the
University of Maryland, College Park in partial fulfillment
of the requirements for the degree of
Doctor of Philosophy
2005

Advisory Committee:

Professor Brian R. Hunt, Chairman/Advisor
Professor Kenneth R. Berg
Professor James A. Yorke
Professor Michael Boyle
Professor Edward Ott, Physics

DEDICATION

To my wonderful family: parents Levertis and Emille Grant, sister Candice Grant and grandmother Jimmie Frazier.

ACKNOWLEDGEMENTS

This dissertation would not have been possible without the terrific support from academic advisors, family and friends.

First, I offer my deepest gratitude and respect for my advisor Dr. Brian Hunt. He taught me a great deal about how to approach a research problem, ask questions and express my ideas in presentations and academic papers. His oral and written advice and comments were always extremely perceptive and helpful. Not only was he continuously available for me even throughout his bout with cancer, he was a tremendous source of support during my own. It was certainly my pleasure to be his student.

Besides my advisor, let me also say a big 'thank you' to Dr. Daniel Rudolph, Dr. James Yorke, Dr. Michael Boyle, Dr. Kenneth Berg and Dr. Edward Ott for their insightful remarks and assistance as members of my preliminary and final oral committees; the staff of the Mathematics Department for their optimism, encouragement and

timely assistance with deadlines; my study partner Dr. Ian Frommer and the rest of the students and faculty of Maryland's Mathematics department for creating such a comfortable working environment.

Special thanks to Dr. M. Christine Jackson for inspiring me (a week before the deadline) to apply to Maryland and to long-time friends Tanya Upthegrove-Coleman, Marianne Ragins-McGee, and roommate/friend Calandra Tate for being my ever-present cheerleaders.

I would also like to acknowledge Dr. Lisa Jacobs, Dr. Navin Singh, Dr. Lee Resta, Physician Assistant Melanie Erb and Oncology Nurse Marybeth Halter for their wonderful care during my treatment at Johns Hopkins.

Finally, the love and support of my entire family has been such a blessing throughout this experience, but I would be remiss if I didn't express some special acknowledgments to my cousin Dr. Monique McRipley for stimulating my interest in pursuing a higher degree in the sciences; my sister Candice Grant for taking such good care of me when I was down and for providing a daily laugh; my grandmother Jimmie Frazier for the numerous thoughtful cards and letters; and last but certainly not least my parents Levertis and Emille Grant for their affection, strength, encouragement and enduring faith in me.

TABLE OF CONTENTS

LIST OF FIGURES

Chapter 1

Introduction

Given a chaotic attractor A, we consider the problem of maximizing over all trajectories $\{x_n\}$ in A the time average

$$\langle F \rangle = \lim_{N \to \infty} \frac{1}{N} \sum_{n=0}^{N-1} F(x_n)$$

of some continuous function $F : A \to \mathbb{R}$, which we call the *performance function*. With mild assumptions, this problem is equivalent to finding an invariant measure μ on A that maximizes

$$\langle F \rangle = \int F(x) d\mu(x).$$

In Chapter 2 we consider this problem for one-dimensional expanding maps and Lipschitz performance functions. We present a method that rigorously constructs a subset S of A for which a trajectory is optimal if and only if it remains within S. Then it finds a (generally unique) periodic orbit contained in S. Though S cannot be determined exactly on a computer, by approximating it we get rigorous upper and lower bounds on the optimal average and find that in practice these bounds are very close to each other. For several examples, we compare our results to the brute force approach of exhaustively searching all periodic orbits up to a given period. We find that the two approaches agree quite

well and that our direct method is many times faster. Our method also applies to expanding maps in higher dimensions.

In Chapter 3, we present a method that is more practical than that of Chapter 2 for higher dimensional systems and does not require the system to be expanding in all directions, though it yields less rigorous information. The method involves examining a trajectory and assigning a score to almost periodic pieces of the trajectory. The piece with the highest score indicates a nearly periodic orbit that is, if not optimal, at least close to optimal. For hyperbolic attractors, the score is a rigorous lower bound on the optimal average. We give examples illustrating the accuracy of the method for both hyperbolic and non-hyperbolic attractors.

Chapter 2

One Dimension

2.1 Introduction

Consider the general problem of optimization on a chaotic attractor A. There are many different definitions of chaos; here we assume at least that A is a compact invariant set that contains a dense set of periodic orbits. By optimization, we mean maximizing the time average

$$\langle F \rangle = \lim_{N \to \infty} \frac{1}{N} \sum_{n=0}^{N-1} F(x_n) \tag{2.1}$$

of some continuous function $F : A \to \mathbb{R}$, over all trajectories $\{x_n\}$ in A for which the limit exits. We call F the *performance function*. For a continuous dynamical system $x_{n+1} = h(x_n)$, maximizing (2.1) is equivalent to maximizing the space average

$$\langle F \rangle = \int F(x) d\mu(x).$$

over all invariant probability measures μ on A for the following reasons. Since A is compact, the set of all invariant probability measures on A is weakly compact, thus there must always be a maximizing measure. Furthermore, one can show [10]

that a maximizing measure μ satisfies

$$\int F d\mu = \sup_x \limsup_{N\to\infty} \frac{1}{N} \sum_{n=0}^{N-1} F(h^n(x)).$$

It then follows from the Birkhoff ergodic theorem that almost every initial condition with respect to μ yields an optimal trajectory.

Many attractors have the property that Lebesgue almost every initial condition in a neighborhood of the attractor yields the same time average $\langle F \rangle$; this is known to be true, e.g., for certain one-dimensional expanding maps [12] and for Axiom A attractors [5, 17], and is believed to be true much more generally. Maximizing a function that is constant almost everywhere may not seem to be of practical importance; here we summarize two motivations given in [9] for studying this problem.

Control of chaos. Unstable periodic orbits within a chaotic attractor can be stabilized with a small amplitude feedback control [7]. Thus, if there is a function measuring the instantaneous performance of the system and a certain unstable periodic orbit is determined to be optimal (i.e., the orbit gives the best average performance) then one can stabilize the system near this orbit and optimize performance.

Chaotically forced systems. Suppose we have two systems B and C such that the dynamics of system C is dependent on that of B:

$$\frac{dx}{dt} = f_B(x); \qquad \frac{dy}{dt} = f_C(x, y).$$

If x evolves on a chaotic attractor, then stability of the y dynamics is influenced by unstable orbits in the x attractor. Consider for example, the case $f_C(x, y) = g(x)y$. If the "transverse" Lyapunov exponent $\langle g(x) \rangle$ is negative for all trajectories of a system B, then the manifold $y = 0$ is asymptotically stable.

But if the transverse Lyapunov exponent is positive for some trajectory of system B, then trajectories of the combined system that start arbitrarily close to $y = 0$ can diverge from it. Similar statements can be made in the case of nonlinear y dynamics; see [1, 2]. In order to anticipate such a loss of stability as system parameters change, it is important to monitor the maximum transverse Lyapunov exponent of all x trajectories, not just the transverse Lyapunov exponent of a typical x trajectory.

Past work on optimal orbits has concentrated on the *type* of orbit that maximizes $\langle F \rangle$, at least for 'typical' A and F. Several results, both rigorous and numerical, suggest that typically the maximum of $\langle F \rangle$ occurs on a periodic orbit [4, 6, 9, 14, 11, 10, 16, 13]. Our concern is instead with how to find an orbit that yields the optimal average for a particular A and F. This may not be practical in cases where the 'optimal orbit' has high period or is non-periodic, though in such cases we will still find rigorous bounds on the optimal average. Fortunately, past work has shown that the answer is usually a periodic orbit with reasonably low period, so we now review this work that provides the basis for our method.

Rigorous and numerical studies of this problem began independently around the same time. Mañé [14] considered the related problem of minimizing the Lagrangian for Lagrangian dynamical systems. Our interest is in the case that the performance function F is independent of the dynamics. In this context, early work centered around the following example, which we also took as our prototype example: the doubling map (denoted here by the function $h_D : \mathbb{T}^1 \to \mathbb{T}^1$)

$$x_{n+1} = h_D(x_n) := 2x_n \quad \text{(modulo 1)}, \tag{2.2}$$

with the one-parameter family of performance function

$$F_\omega(x) = \cos[2\pi(x - \omega)]. \tag{2.3}$$

For a given ω, the question is which orbit of (2.2) gives the greatest value of $\langle F_\omega \rangle$.

For the example above, Jenkinson [11] conjectured that for Lebesgue almost every ω, there is a unique optimal invariant measure supported on a periodic orbit. This conjecture was proved by Bousch [4]. Meanwhile, Hunt and Ott [9] studied numerically the same example, and other examples with different chaotic maps and performance functions. They conjectured more generally that typically there is an optimal periodic orbit, based on the observation that in the numerical experiments, a low period orbit was optimal for most parameter values. The experiments employed a 'brute force' approach, finding all periodic orbits of (2.2) up to period 24 (there are $\sim 10^6$ such orbits), then calculating and comparing the value of $\langle F_\omega \rangle$ over each of these orbits to determine which one produced the optimal average. While this method is likely to yield an optimal orbit, and otherwise a near-optimal orbit, it requires finding all the periodic orbits of the system up to a given period. This approach may be quite difficult and computationally expensive for a general chaotic system, and yields no rigorous information about whether the orbit found is actually optimal or how close to optimal it is.

In this paper we describe a method that, for continuous expanding maps of the circle and Lipschitz performance functions, directly computes an optimal orbit in a rigorous manner. Our method involves finding the fixed point of a contracting functional operator, which we do in practice by iterating the operator. While we cannot find the fixed point by any finite computation, we can still obtain a rigorous bound an how close to optimal the orbit found is. By increasing the resolution of our approximation to the functional operator, we can make this bound as small as we like.

Figure 2.1 qualitatively compares our method at a moderate resolution to the

aforementioned brute force method for the prototype example. For each of 10,000 equally spaced values for the parameter ω, we plotted the period of the orbit of (2) that gave us the optimal average value of (3). Although these graphs do appear to be somewhat different (for the higher period orbits in particular), our method actually differs from the brute force method for only 0.01% of the parameter values. Further details of these experiments will be discussed in Section 3.

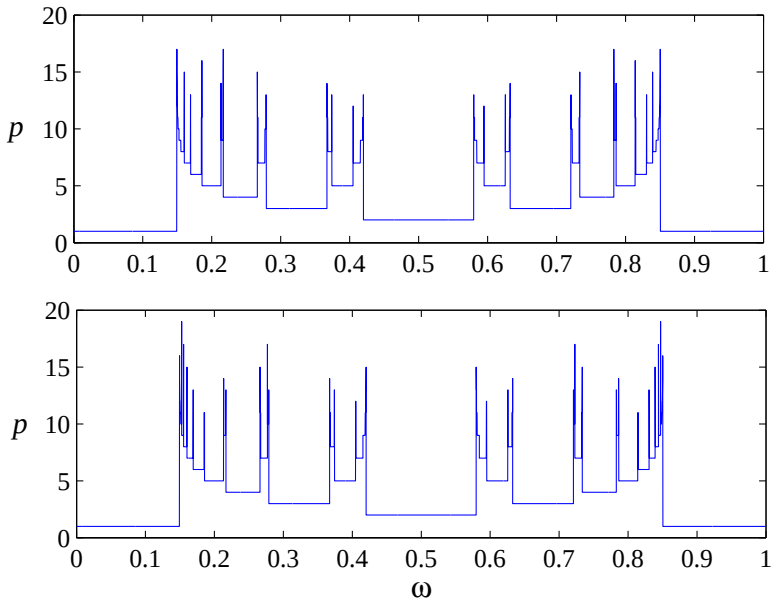

Figure 2.1: Optimal period p for (2.2), (2.3) as a function of ω for 10,000 evenly spaced values for the parameter ω, using our method (upper graph) with a grid resolution of 20,000 grid points and the brute force method (lower graph), which checks every periodic orbit up to period 24 for each parameter value.

The rest of the chapter shall proceed as follows. In Section 2, we present our method and its rigorous basis. We discuss the implementation of our method in Section 3 and compare our results to those of the 'brute force' method for a

variety of systems. In Section 4 we give a brief summary.

2.2 Optimization Method and Justification

The essence of our method is as follows. Given a continuous map h, an invariant set A for h, and a continuous function F from A to $\mathbb{R}$, construct a continuous function G such that

$$\tilde{F}(x) = F(x) + G(x) - G(h(x)) \tag{2.4}$$

is equal to its maximum value M on a large enough set to contain a trajectory of h (equivalently, to support an invariant measure of h). Then M is the maximum of $\langle \tilde{F} \rangle$, and every trajectory (or invariant measure) contained in the set where $\tilde{F}(x) = M$ is optimal. These trajectories (measures) are optimal for $\langle F \rangle$ because $\langle \tilde{F} \rangle = \langle F \rangle$ for *all* trajectories.

Although we may not be able to compute such a G and $\tilde{F}$ exactly, finding a G for which the maximum value of $\tilde{F}$ is close to its maximum average can still give good rigorous bounds on the $\langle F \rangle$. The following proposition follows trivially from the relation $\langle \tilde{F} \rangle = \langle F \rangle$.

Proposition 2.1. *For any continuous function G, the maximum of $\langle F \rangle$ is bounded above by the maximum value of $\tilde{F}$ and below by its average over any periodic orbit.*

In the case that h is an expanding map of the circle, we can generally obtain a periodic orbit that yields a good lower bound by iterating h backward and always choosing the pre-image that gives the larger value of $\tilde{F}$.

The existence of a G for which the maximum of $\tilde{F}$ is equal to the maximum average is guaranteed in a variety of settings (i.e., certain hypotheses on h, A, and

F) [4, 6, 13, 14, 16]. These statements are sometimes called "non-positive Livsic Theorems." In general, the statement of a such a theorem has the following form:

Theorem. *With appropriate hypotheses on h, A, and F, if $\langle F \rangle \leq M$ for all invariant measures on A, then there exists a continuous function G_* such that*

$$F(x) + G_*(x) - G_*(h(x)) \leq M \tag{2.5}$$

for all x in A.

If h is the time-one map of a Lagrangian flow and if $-F$ is the Lagrangian [14] or if h is the doubling map and f is Lipschitz [4], then the function G_* satisfying (2.5) is Lipschitz. If F is Hölder continuous, then so is G_* (possibly with a different exponent) for $C^{1+\alpha}$ expanding maps [6], C^2 Anosov diffeomorphisms [13] or Anosov flows [16].

Notice that G_* is not uniquely determined by the conditions of such a theorem. In particular, if $\tilde{F}(x) = F(x) + G_*(x) - G_*(h(x)) < M$, then G_* can be increased slightly near x without affecting (2.5). Our interest is in a practical method to construct an appropriate G_* for a given h and F and we describe here such a method in the case that h and F are functions on the circle $\mathbb{T}^1$ with h (uniformly) expanding (that is, $|h(x) - h(y)| \geq C|x - y|$ for some $C > 1$ and $|x - y|$ sufficiently small) and F Lipschitz. If in addition h is $C^{1+\alpha}$, the existence of a Hölder continuous G_* is a result of Contreras, Lopes and Thieullen [6]. However, we found it impractical to compute $G_*(x)$ according to their definition, since it requires considering all backward trajectories from x. Instead, we determine a Lipschitz G_* as a fixed point of a contracting functional operator ϕ, thereby generalizing Bousch's technique [4], and compute G_* by iterating ϕ.

We have the following result:

Proposition 2.2. *Let h be a continuous expanding map on $\mathbb{T}^1$, and let $F : \mathbb{T}^1 \to \mathbb{R}$ be Lipschitz. Then the functional operator ϕ defined by*

$$\phi(G)(y) = \max_{h(x)=y} (G + F)(x)$$

is contracting (not necessarily strictly) on the space $C(\mathbb{T}^1, \mathbb{R})$ with the uniform metric. Furthermore, ϕ has a fixed point in the quotient space of Lipschitz functions from $\mathbb{T}^1$ to $\mathbb{R}$ modulo constant functions; equivalently, there are a Lipschitz function G_* and a constant M such that $\phi(G_*) = G_* + M$. This G_* and M satisfy (2.5) *for all $x \in \mathbb{T}^1$, and M is the maximum of $\langle F \rangle$.*

Proof. There are four parts to the proof. We show that:

a) The operator ϕ is a (not necessarily strict) contraction in the uniform metric;

b) For K sufficiently large, if G is K-Lipschitz (that is, Lipschitz with constant K), then so is $\phi(G)$;

c) Factoring out the constant functions yields a compact space on which ϕ has a fixed point;

d) The constant $M = \phi(G_*) - G_*$ is the maximum of $\langle F \rangle$.

For part (a), let $\| \cdot \|$ denote the L^∞ norm, and consider continuous functions G, G' with $\|G - G'\| = \delta$. Then for some $y^* \in \mathbb{T}^1$,

$$\begin{aligned} \|\phi(G) - \phi(G')\| &= |\phi(G)(y^*) - \phi(G')(y^*)| \\ &= |\max_{h(x)=y^*} (G + F)(x) - \max_{h(x)=y^*} (G' + F)(x)| \\ &= |G(x_1) + F(x_1) - (G'(x_2) + F(x_2))| \end{aligned}$$

where x_1 and x_2 are (possibly equal) pre-images of y^*. Then

$$G(x_1) + F(x_1) - (G'(x_2) + F(x_2)) \leq$$
$$G(x_2) + F(x_2) - (G'(x_2) + F(x_2)) = G(x_2) - G'(x_2) \leq \delta$$

and

$$G(x_1) + F(x_1) - (G'(x_2) + F(x_2)) \geq$$
$$G(x_1) + F(x_1) - (G'(x_1) + F(x_1)) = G(x_1) - G'(x_1) \geq -\delta,$$

so that $\|\phi(G) - \phi(G')\| \leq \delta$.

For part (b), let G be K-Lipschitz; we need to specify K so that this implies $\phi(G)$ is K-Lipschitz. Let K_F denote the Lipschitz constant of F. Choose $y_1, y_2 \in \mathbb{T}^1$ and assume without loss of generality that $\phi(G)(y_1) \geq \phi(G)(y_2)$. Let x_1 be the pre-image of y_1 at which $\phi(G)(y_1) = F(x_1) + G(x_1)$. Since h is expanding, there is a constant $c_h > 1$ independent of y_1 and y_2 such that y_2 has a pre-image x_2 with $|y_1 - y_2| \geq c_h|x_1 - x_2|$. Then $\phi(G)(y_2) \geq F(x_2) + G(x_2)$, and hence

$$\begin{aligned}
|\phi(G)(y_1) - \phi(G)(y_2)| &= \phi(G)(y_1) - \phi(G)(y_2) \\
&\leq F(x_1) + G(x_1) - (F(x_2) + G(x_2)) \\
&\leq |F(x_1) - F(x_2)| + |G(x_1) - G(x_2)| \\
&\leq K_F|x_1 - x_2| + K|x_1 - x_2| \\
&= (K_F + K)|x_1 - x_2| \\
&\leq \frac{(K_F + K)}{c_h}|y_1 - y_2|.
\end{aligned}$$

Thus if G is K-Lipschitz with $K = K_F/(c_h - 1)$, then $\phi(G)$ is K-Lipschitz too because then $(K_F + K)/c_h = K$.

To show part (c), let W be the space of Lipschitz functions from $\mathbb{T}^1$ to $\mathbb{R}$, and let $\overline{W}$ be the quotient space of W modulo the constant functions. Notice

that $\overline{W}$ is a Banach space with the norm of $\overline{G} \in \overline{W}$ being the infimum of all Lipschitz constants for $\overline{G}$. The K-Lipschitz functions form a compact subset of $\overline{W}$ by the Ascoli-Arzelà Theorem. Since this set is also convex, by the Schauder Fixed Point Theorem, $\overline{\phi}$ has a fixed point $\overline{G}_*$.

Let $G_* \in W$ be an element in the equivalence class of $\overline{G}_*$. Then $\phi(G_*) = G_* + M$ for some constant M, or in other words

$$\max_{h(x)=y} (G_* + F)(x) = G_*(y) + M \tag{2.6}$$

for all $y \in \mathbb{T}^1$. Then

$$G_*(x) + F(x) \leq G_*(h(x)) + M$$

G_* satisfies (2.5). Taking the average of (2.5) over any trajectory, we have $\langle F \rangle \leq M$.

Finally, to establish that M is the maximum of $\langle F \rangle$, we argue that there is a nonempty invariant subset of the set nonempty $S = \{x : F(x) + G_*(x) - G_*(h(x)) = M\}$; then every trajectory in this invariant subset has $\langle F \rangle = M$. Notice that if $y \in S$, then by equation (2.6), it has a preimage x such that $G_*(x) + F(x) = G_*(y) + M = G_*(h(x)) + M$; that is, $x \in S$. By induction, there is an infinite backward trajectory of h that remains in S. The limit set of this backward trajectory is invariant and is contained in S since S is closed. □

Therefore if $\tilde{F}(x) = F(x) + G_*(x) - G_*(h(x))$ and M is the maximum value of $\tilde{F}$, we would like to find a trajectory of h that stays inside the set $S = \{x : \tilde{F}(x) = M\}$.

Our method proceeds as follows:

Step 1: *Find an approximation to* G_*. The iteration $G_{n+1} = \phi(G_n) - C_n$ (where $C_n = \min(\phi(G_n))$, so that each G_n has a minimum of zero) seems like a

reasonable procedure, but since ϕ is not a strict contraction, we run the risk of obtaining a periodic sequence of G_n's instead of a fixed point. To increase our chances of converging to a fixed point, we replace ϕ with the (still contracting) iteration $G_{n+1}(x) = (\phi(G_n(x)) + G_n(x))/2 - C_n$ again choosing C_n to make $\min(G_{n+1}) = 0$. We stop when G_{n+1} is uniformly within some pre-specified tolerance ϵ of G_n, and let $\hat{G}_* = G_{n+1}$ be our approximation to G_*.

Step 2: *Let $\tilde{F}(x) = F(x) + \hat{G}_*(x) - \hat{G}_*(h(x))$ and iterate the map h backward, always choosing the preimage for which $\tilde{F}$ is the largest.* In other words, we perform backward iteration in the set $S^{\wedge} = \{x : \tilde{F}(x) \geq \tilde{F}(z)$ whenever $h(x) = h(z)\}$. If $\hat{G}_*$ were equal to G_*, then $S^{\wedge}$ would be the same as S defined above.

Step 3: *Obtain an "optimal" unstable periodic orbit.* Since h is an expanding map, this procedure will quickly converge to an unstable invariant set.

In practice we always found Step 3 to yield an unstable periodic orbit, and this orbit is our method's candidate for the optimal orbit. In addition, recalling Proposition 1.1, the average M_- of F over our candidate orbit is a lower bound on M, and the maximum value M_+ of $\tilde{F}$ is an upper bound on M. The more accurately we approximate G_*, the closer these bounds will be.

2.3 Experimental Results

To see how our method works in practice, we compared it to the results from the 'brute force' method for several examples studied in [9]. We now make some general remarks about comparisons with the brute force method. Unless otherwise

specified, we used a grid of 20,000 points for the calculation of the functions G_n, and stopped when G_n and G_{n+1} came within $\epsilon = 10^{-6}$ of each other. We also varied these parameters in some cases to see their effect on the results. When we require a value of G_n between grid points, we compute it with linear interpolation.

Let M_p be the maximum of $\langle F \rangle$ over all periodic orbits of h with period at most p. Notice that $M_p \leq M$, with equality if there is an optimal orbit of period at most p. In each case, we compare the results of our method to M_{24} for a one-parameter family $\{F_\omega\}$ of performance functions using 10,000 evenly spaced values of the parameter ω.

In cases when the two methods disagree, our method generally finds a different periodic orbit with period less than 25, which we then know is not optimal. Given that both methods find orbits with period much less than 25 for most values of ω, we believe that we have found a true optimal orbit in virtually all cases that the two methods agree.

2.3.1 Prototype Example

For the prototype example, the doubling map (2.2) with sinusoidal performance function (2.3) we can qualitatively see the results of the experiment described above in Figure 2.1 where we plot the optimal period found by both methods versus the parameter ω. Notice that, the optimal orbit is constant over intervals of parameter space. The only places where our method doesn't agree with the brute force method are close to transitions in parameter space from one optimal period to another.

Our main results for this example are as follows:

- Our method's result agrees with the brute force method for over 99% of

the parameter values. By increasing N (the grid size for the G_n iteration), we could obtain agreement for each of the parameter values that yielded a discrepancy with a grid size of $N = 20,000$ points.

- The orbit we obtained with our default values of $N = 20,000$ and $\epsilon = 10^{-6}$ always yielded a value of $\langle F_\omega \rangle$ within 0.00003 of the optimal average found by brute force, a more than adequate result for improving performance in the controlling chaos scenario.

- For these particular experiments our method ran more than 50 times as fast as the 'brute force' method (0.059 seconds per ω versus 3.8 seconds per ω).

In Fig. 2.2, we compare for all ω the lower and upper bounds M_- and M_+ that we obtain with the brute force maximum average M_{24}. When we plot the differences $M_- - M_{24}$ and $M_+ - M_{24}$ we see some very small discrepancies. For 98.97% of the parameter values ω, both the upper and lower average come within 10^{-6} of the true optimal average. The lower bound M_- is equal to M_{24} for 99.82% of the parameter values.

We now explore the effect in this example of varying the threshold ϵ and the grid size N used to calculate $\hat{G}_*$. Of course a smaller ϵ and greater N will improve the accuracy of our results, but also will increase the computation time. Tables 2.1 and 2.2 show the effect of varying N and ϵ on our method for the prototype example. We don't have a dramatic increase in computation time, nor do we gain much in accuracy by decreasing the value of ϵ.

Varying the grid size N has a more significant effect on timing and accuracy. The larger N is, the closer the region $\hat{S}$ in which we iterate h backward will be

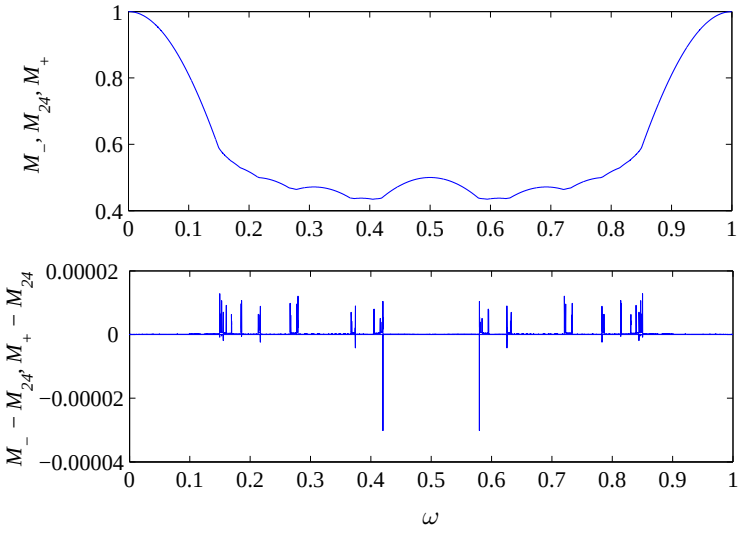

Figure 2.2: For the doubling map with performance function $\cos[2\pi(x-\omega)]$ and 10,000 equally spaces values of the parameter ω, we compare of the lower and upper bounds M_- and M_+ yielded by our method and the maximum average M_{24} found by brute force. The upper graph shows all three quantities as a function of ω. On the given scale, these quantities are indistinguishable. In the lower graph, we plot the differences $M_- - M_{24}$ and $M_+ - M_{24}$ between the upper and lower bounds and the brute force average. The bounds are always within 0.00004 of each other, and for most ω are much closer than that.

ϵ	% Agreement	Max. $(M_+ - M_-)$	Avg. Computation Time
10^{-4}	99.70	0.00004997	0.037 sec/ω
10^{-6}	99.82	0.00003015	0.059 sec/ω
10^{-8}	99.84	0.00003015	0.072 sec/ω

Table 2.1: Varying the iteration threshold ϵ does not have as significant effect on the accuracy our results compared to the results found by brute force. Each of these trials was performed on the prototype example with 10,000 evenly spaces values of the parameter ω and a grid size of $N = 20,000$. The second column gives the percentage of ω values for which both methods find the same orbit, and thus M_- and M_{24} agree. The third column gives the maximum value of $M_+ - M_-$ over all ω, and the fourth column gives the average computer time per ω value on a 2.8GHz Intel P4 Xeon processor.

to the correct region $S = \{x : \tilde{F}(x) = M\}$. Even a small discrepancy can change the orbit we find, especially in the case where the period of the optimal orbit is high, because then it is more likely to have points close to the boundary of S. As expected, we do see improvement in Table 2.2 as the grid size increases. The computation time grows slightly faster than linearly with N.

2.3.2 Other Examples

Consider first the case of the doubling map with multi-humped performance function $F_\omega(x) = \cos[2\pi(x-\omega)]+\sin[6\pi(x-\omega)]$. Figures 2.3 and 2.4, show the optimal period and error bound differences, respectively. Overall, the periods agree (and $M_- = M_{24}$) for 99.86% of the values of ω. Thus we have accuracy similar to the prototype example with this more complicated performance function.

N	% Agreement	Max. $(M_+ - M_-)$	Avg. Computation Time
80,000	99.96	0.00000246	0.32 sec/ω
40,000	99.90	0.00000739	0.15 sec/ω
20,000	99.82	0.00003015	0.059 sec/ω
5,000	99.60	0.00010379	0.011 sec/ω
1,000	98.60	0.00064012	0.0022 sec/ω

Table 2.2: The effect of N (the size of the grid used to calculate $\hat{G}_*$) for the prototype example. For all these trials we used 10,000 evenly spaced values for the parameter ω. The max bound error column gives the larger of the upper bound error and lower bound error over all ω and iteration threshold $\epsilon = 10^{-6}$. The second, third, and fourth columns are as in Table 2.1. The average computation time for the brute force method was 3.8 seconds/ω.

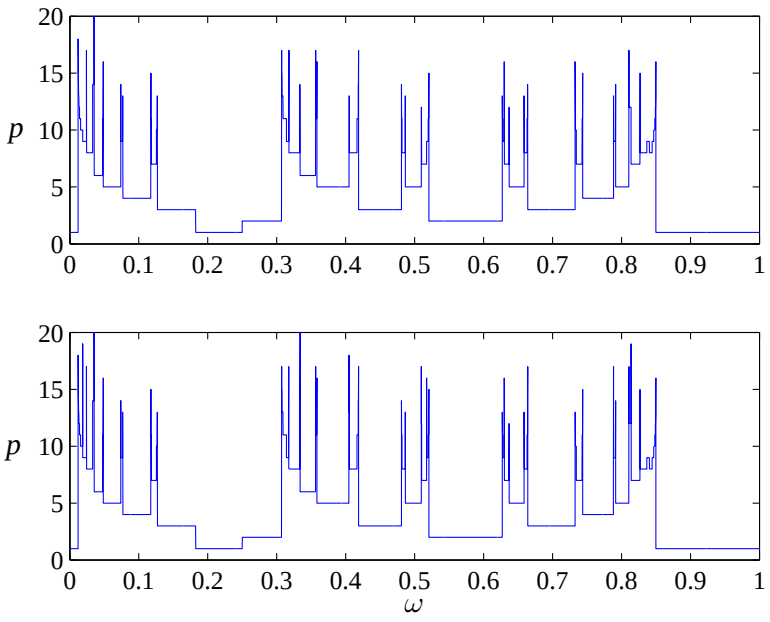

Figure 2.3: The optimal period obtained from our method (upper graph) and the brute force method (lower graph) for the doubling map using the performance function $F_\omega(x) = \cos[2\pi(x-\omega)] + \sin[6\pi(x-\omega)]$.

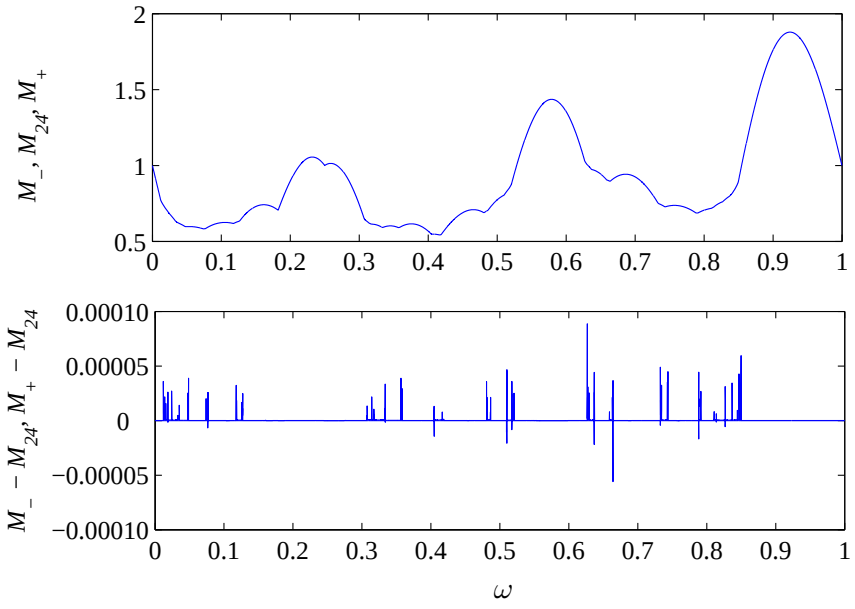

Figure 2.4: Optimal average and differences, as in Fig. 2.2, for the doubling map with the performance function $F_\omega(x) = \cos[2\pi(x-\omega)] + \sin[6\pi(x-\omega)]$.

Consider next replacing the doubling map h_D the tent map $h_T(x) = 1 - |2x - 1|$. Though not strictly expanding according to our definition in Section 2.2, the proof of Proposition 2.2 still applies. Using the same performance function (2.3) as in the prototype example, we see in Figure 2.5 that there are significantly fewer parameter values with high period optimal orbits. The two methods agree quite well, differing only at eight values of ω. The spikes seen around $\omega = 0.15$ in Fig. 2.6 coincide to the beginning of the cascade in Fig. 2.5. Otherwise, even the upper bound remains within 0.000002 of the optimal average. We summarize the results of these variations in Table 2.3.

Next we consider the case of a chaotic map that is not uniformly expanding, using the logistic map $h_Q(x) = 4x(1-x)$. We estimated the optimal average

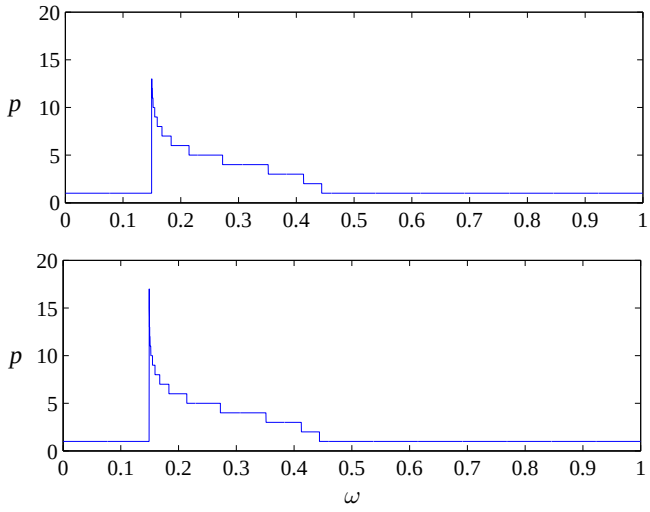

Figure 2.5: The optimal period obtained from our method (upper graph) and the brute force method (lower graph) for the tent map $= 1-|2x-1|$ with performance function $F_\omega(x) = \cos[2\pi(x-\omega)]$.

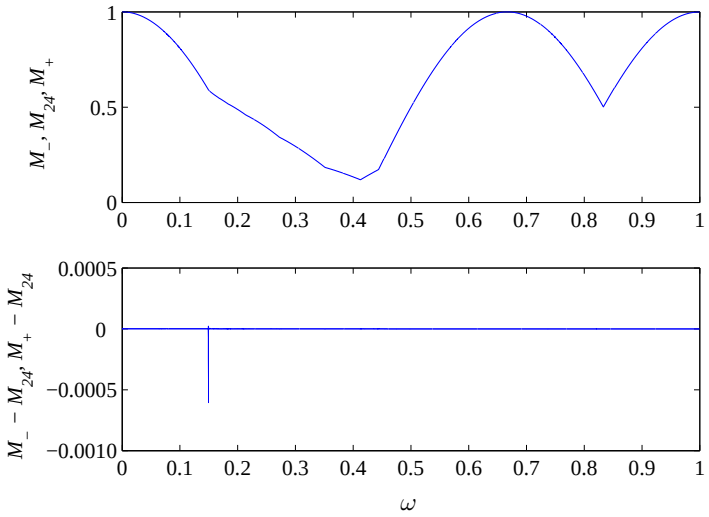

Figure 2.6: Optimal average and differences, as in Fig 2.2 for the tent map with performance function $F\omega(x) = \cos[2\pi(x-\omega)]$.

Map	Perf. Function	% Agreement	Max. $(M_+ - M_-)$
$x_{n+1} = 2x_n$	$\cos[2\pi(x-\omega)]$	99.82	0.00003015
	$\cos[2\pi(x-\omega)]$ $+\sin[6\pi(x-\omega)]$	99.86	0.00008874
$x_{n+1} = 1 - \lvert 2x_n - 1\rvert$	$\cos[2\pi(x-\omega)]$	99.92	0.00060700

Table 2.3: Results for other chaotic systems and performance functions. We use the our standard values of $N = 20,000$ and $\epsilon = 10^{-6}$ and 10,000 evenly spaced values of the parameter ω.

in two ways. First, we directly used the method described in Section 1.2 on $h_Q(x) = 4x(1-x)$ using performance function $F_\omega = \cos[2\pi(x-\omega)]$. With this approach, Proposition 2.2 does not guarantee convergence of the iteration that produces $\hat{G}_*$, but nonetheless we did find the iteration to converge in practice. Regardless of the method we use to find $\hat{G}_*$, Proposition 2.1 still applies and the bounds M_- and M_+ we obtain are rigorous, up to the precision of the computer.

Secondly, by using the fact that the logistic map is conjugate to the tent map, $h_T(x) = 1 - |2x-1|$, and transforming the performance function through the conjugacy function, we applied the method to the tent map paired with the transformed performance function. Specifically, with the function $\psi(x) = (1-\cos\pi x)/2$, we have $h_Q \circ \psi(x) = \psi \circ h_T(x)$ and for every performance function F,

$$\begin{aligned} F \circ h_Q^i(x) &= F \circ (\psi \circ h_T \circ \psi^{-1})^i(x) \\ &= F \circ (\psi \circ h_T^i \circ \psi^{-1})(x) \\ &= (F \circ \psi) \circ h_T^i(\psi^{-1}(x)). \end{aligned}$$

Thus the average of F over a trajectory of h_Q is the average of $F \circ \psi$ over a trajectory of h_T. So we apply the method to the tent program using the performance function $F_\omega \circ \psi(x) = \cos[\pi(1 - \cos \pi x) - 2\pi\omega]$.

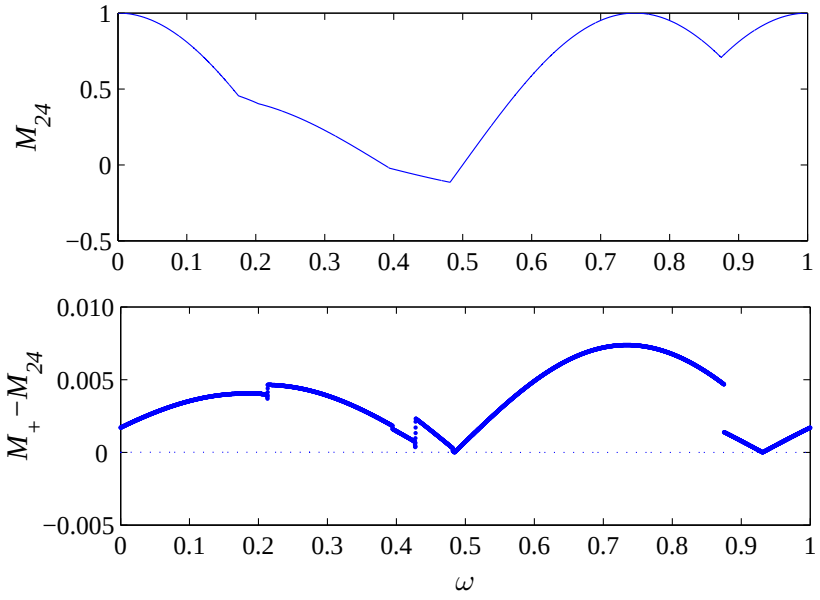

Figure 2.7: The logistic map h_Q yields a brute force optimal average (upper graph) similar to that of the tent map h_T (Fig. 2.6). The lower graph shows the difference between the optimal average found by brute force and the upper bound results from our two methods; the dashed curve is the result of using h_T and the transformed performance function, while the darker curve comes from direct application of our method to h_Q. In the former case, the largest value of $M_+ - M_{24}$ is 2.11×10^{-6}. In both cases the periodic orbit we obtain agrees with the brute force method, and thus $M_- = M_{24}$, for all ω.

Using both approaches, we found the same optimal orbit as the brute force method for all values of ω; the optimal period was always at most 4. The differ-

ence between the two ways in which we applied our method is the quality of upper bounds we obtained, as seen in Fig. 2.7. While applying our method directly to a non-expanding map can produce the correct optimal orbit, the upper and lower bounds we obtain are not as close to each other as in the expanding case.

2.4 Conclusion

In this chapter we have described a practical, efficient method for optimizing the time average of a function over trajectories of an expanding map on the circle. If the optimal trajectory is a periodic orbit with relatively low period, our method finds the orbit very quickly. While not proving the orbit to be optimal, it provides a rigorous upper bound on the optimal average indicating that the orbit is at least very close to optimal.

Our method can also find high period optimal orbits, when used with sufficient computational resolution. Furthermore, it can be applied to chaotic maps that are not uniformly expanding, though the rigorous bounds it obtains on the optimal average are less precise.

While we have focused on one-dimensional maps, our method and Proposition 2.2 apply also to expanding maps in higher dimensions. However, iteration of the functional operator ϕ becomes computationally more difficult and time consuming as the dimension increases. For higher dimensional chaotic maps with a low-dimensional attractor, a different approach seems more practical. We consider this in Chapter 3.

Chapter 3

Higher Dimensions

3.1 Introduction

In the previous chapter we concentrated on one-dimensional expanding maps. Most of the physical systems where maximizing such an average is useful occur in higher dimensions. Our one dimensional method is difficult to extend to systems in higher dimensions that are not uniformly expanding, for a few reasons. Most importantly, if the system has contracting directions, then the operator ϕ used in our one-dimensional method either does not have fixed point, or the fixed point is sufficiently non-smooth that it is difficult to approximate on the computer due to finite resolution.

In this chapter we describe a higher dimensional method that is both efficient and easy to use, yet has some theoretical foundation. The method uses only the performance function and a finite-length trajectory, and thus can be used even for experimental systems in which the exact dynamics are unknown. We obtain at least an approximation to a near-optimal periodic orbit and, for hyperbolic systems, a rigorous lower bound on the actual optimal average.

Our method is as follows. Given a trajectory $\{z_0, z_1, \ldots z_n\}$ on a chaotic attractor and a Lipschitz performance function F, with Lipschitz constant M, compute for each trajectory segment $\{z_n, z_{n+1}, \ldots z_{n+p}\}$ with $0 \leq n < n+p \leq N$ the "score"

$$S(n,p) = \frac{1}{p}\left[\sum_{k=0}^{p-1} F(z_{n+k}) - MC|z_n - z_{n+p}|\right]. \tag{3.1}$$

(In practice we speed up computation by only considering values of p up to some maximum value, specifically 20 for the results we show.) Here C is a constant that depends on the attractor; in the case of a hyperbolic attractor, the Anosov Closing Lemma implies that one can determine C such that if $|z_n - z_{n+p}|$ is sufficiently small, there is a period p orbit near $\{z_n, \ldots, z_{n+p-1}\}$ on which the average of F is at least $S(n,p)$. We then maximize $S(n,p)$ to obtain a rigorous lower bound on the optimal average. Our method suggests that the optimal orbit has period p and lies close to the maximizing piece $\{z_n, \ldots, z_{n+p-1}\}$ of the given trajectory. Even when the attractor is not hyperbolic, one can apply our method, though it yields no rigorous information and the results depend on the choice of the constant C.

In Section 2 we describe the rigorous basis of our method and give an example of how to determine C for a hyperbolic attractor. In Section 3, we present results of applying our method in both a hyperbolic case, the Kaplan-Yorke attractor an a non-hyperbolic case, the Hénon attractor. In the latter case, we discuss how to choose a reasonable value of C empirically.

3.2 Method for Hyperbolic systems

The theoretical basis for our method is the Anosov Closing Lemma. The formulation below is implied by the treatment of this result in [8].

Theorem (Anosov). *A hyperbolic set for a diffeomorphism h has a neighborhood V and a constants C, $\epsilon_0 > 0$ such that if $h^i(z) \in V$, $0 \leq i \leq p$, and $\epsilon = |h^p(z) - z| \leq \epsilon_0$, then there is a periodic point z^* with period p (or some factor of p) such that $\sum_{k=0}^{p-1} |h^k(z) - h^k(z^*)| \leq C\epsilon$.*

A hyperbolic set is a compact invariant set that, roughly speaking, has well-defined contracting and expanding directions at each point. The constant C depends on the constants that bound the contraction and expansion rates away from 1, and the minimum angle between the contracting and expanding directions. Here we show how to determine C for a specific class of hyperbolic systems. The systems we consider are hyperbolic on the entire space, so ϵ can be arbitrarily large. They are not diffeomorphisms, but this is not an obstacle.

Specifically, we consider a map h on $\mathbb{T}^1 \times \mathbb{R}$ governed by the equations

$$x_{n+1} = \mu x_n \pmod 1; \tag{3.2a}$$

$$y_{n+1} = \lambda y_n + g(x_n), \tag{3.2b}$$

with $\mu > 1$ a positive integer, $0 < \lambda < 1$ and g a Lipschitz function with Lipschitz constant L. Notice that by induction on k,

$$y_{n+k} = \lambda^k y_n + \sum_{i=0}^{k-1} \lambda^i g(x_{n+k-i-1}).$$

Given a trajectory $(x_0, y_0), (x_1, y_1) \ldots$ of (3.2) the following proposition determines how close a segment $(x_n, y_n), (x_{n+1}, y_{n+1}), \ldots, (x_{n+p}, y_{n+p})$ of the trajectory is to a periodic orbit of period p.

Proposition 3.1. *For every $n \geq 0$ and $p \geq 1$, there is a period p orbit $\{(x_0^*, y_0^*), (x_1^*, y_1^*), \ldots (x_{p-1}^*, y_{p-1}^*)\}$ such that*

$$\sum_{k=0}^{p-1}(|x_{n+k} - x_k^*| + |y_{n+k} - y_k^*|) \leq C_1|x_{n+p} - x_n| + C_2|y_{n+p} - y_n|$$

where $C_1 = [1 + L/(1-\lambda)]/(\mu - 1)$ and $C_2 = 1/(1-\lambda)$.

Note: Whenever we take the absolute value of an x value, we mean its magnitude modulo 1; that is, $|x|$ means the distance from x to the nearest integer.

Proof. First choose δ as close to zero as possible such that

$$(\mu^p - 1)\delta = x_n - x_{n+p} \pmod 1,$$

then $|\delta| = |x_n - x_{n+p}|/(\mu^p - 1)$. Let $x_0^* = x_n + \delta$ and $x_k^* = \mu^k x_0^* \pmod 1$. Then,

$$x_p^* = \mu^p x_0^* = \mu^p x_n + \mu^p \delta = x_{n+p} + x_n - x_{n+p} + \delta = x_0^*.$$

Next, setting

$$y_0^* = \frac{1}{1-\lambda^p}\sum_{i=0}^{p-1}\lambda^i g(x_{p-i-1}^*),$$

and adopting the notation $(x_k^*, y_k^*) = h^k(x_0^*, y_0^*)$, we have

$$\begin{aligned} y_p^* &= \lambda^p y_0^* + \sum_{i=0}^{p-1}\lambda^i g(x_{p-i-1}^*) \\ &= \lambda^p y_0^* + (1-\lambda^p)y_0^* = y_0^*. \end{aligned}$$

Thus (x_0^*, y_0^*) has period p.

Now let $\epsilon_1 = |x_n - x_{n+p}|$ and $\epsilon_2 = |y_n - y_{n+p}|$. Then

$$|x_n - x_0^*| = |\delta| = \frac{1}{\mu^p - 1}\epsilon_1, \tag{3.3}$$

and

$$\begin{aligned} y_{n+p} - y_0^* &= \lambda^p y_n - \lambda^p y_0^* + \sum_{k=0}^{p-1} \lambda^k g(x_{n+p-k-1}) - \sum_{k=0}^{p-1} \lambda^k g(x^*_{p-k-1}) \\ &= \lambda^p (y_n - y_0^*) + \sum_{k=0}^{p-1} \lambda^k [g(x_{n+p-k-1}) - g(x^*_{p-k-1})]. \end{aligned}$$

Writing $y_{n+p} - y_0^* = (y_{n+p} - y_n) + (y_n - y_0^*)$, this implies

$$(1-\lambda^p)(y_n - y_0^*) = y_n - y_{n+p} + \sum_{k=0}^{p-1} \lambda^k [g(x_{n+p-k-1}) - g(x^*_{p-k-1})]$$

so that

$$\begin{aligned} |y_n - y_0^*| &\le \frac{1}{1-\lambda^p} \left[\epsilon_2 + \sum_{k=0}^{p-1} \lambda^k |g(x_{n+p-k-1}) - g(x^*_{p-k-1})| \right] \\ &\le \frac{1}{1-\lambda^p} \left[\epsilon_2 + L|x_n - x_0^*| \sum_{k=0}^{p-1} \lambda^k \mu^{p-k-1} \right] \\ &= \frac{1}{1-\lambda^p} \left[\epsilon_2 + \frac{L\mu^{p-1}\epsilon_1}{\mu^p - 1} \sum_{k=0}^{p-1} \left(\frac{\lambda}{\mu} \right)^k \right] \\ &= \frac{1}{1-\lambda^p} \left[\epsilon_2 + \frac{L\mu^{p-1}\epsilon_1}{\mu^p - 1} \left(\frac{1-(\lambda/\mu)^p}{1-(\lambda/\mu)} \right) \right] \\ &= \frac{\epsilon_2}{1-\lambda^p} + \frac{L(\mu^p - \lambda^p)}{(1-\lambda^p)(\mu^p - 1)(\mu - \lambda)} \epsilon_1. \end{aligned} \tag{3.4}$$

Equations (3.3) and (3.4) show us that when $\epsilon_1 = |x_{n+p} - x_n|$ and $\epsilon_2 = |y_{n+p} - y_n|$ are small, we can be assured that $|x_n - x_0^*|$ and $|y_n - y_0^*|$ are small too. Since periodic orbits in this system are unstable, we can't expect to stay close to the periodic orbit for long. Yet

$$\sum_{k=0}^{p-1} |x_{n+k} - x_k^*| \le \sum_{k=0}^{p-1} \mu^k |x_n - x_0^*| = \frac{\mu^p - 1}{\mu - 1} |x_n - x_0^*| = \frac{\epsilon_1}{\mu - 1} \tag{3.5}$$

and

$$\sum_{k=0}^{p-1} |y_{n+k} - y_k^*| \le \sum_{k=0}^{p-1} \left(\lambda^k |y_n - y_0^*| + L \sum_{i=0}^{k-1} \lambda^i |g(x_{n+k-i-1}) - g(x^*_{k-i-1})| \right)$$

$$
\begin{aligned}
&\leq \sum_{k=0}^{p-1} \left(\lambda^k |y_n - y_0^*| + L|x_n - x_0^*| \mu^{k-1} \sum_{i=0}^{k-1} \left(\frac{\lambda}{\mu} \right)^i \right) \\
&= \frac{1-\lambda^p}{1-\lambda} |y_n - y_0^*| + L|x_n - x_0^*| \sum_{k=0}^{p-1} \mu^{k-1} \left(\frac{1-(\lambda/\mu)^k}{1-\lambda/\mu} \right) \\
&\leq \frac{1-\lambda^p}{1-\lambda} \frac{1}{1-\lambda^p} \left(\epsilon_2 + L\epsilon_1 \frac{\mu^p - \lambda^p}{(\mu^p - 1)(\mu - \lambda)} \right) + \frac{L|x_n - x_0^*|}{\mu - \lambda} \sum_{k=0}^{p-1} \left(\mu^k - \lambda^k \right) \\
&= \frac{1}{1-\lambda} \left(\epsilon_2 + L\epsilon_1 \frac{\mu^p - \lambda^p}{(\mu^p - 1)(\mu - \lambda)} \right) + \frac{L\epsilon_1}{(\mu^p - 1)(\mu - \lambda)} \sum_{k=0}^{p-1} \left(\mu^k - \lambda^k \right) \\
&= \frac{\epsilon_2}{1-\lambda} + L\epsilon_1 \frac{\mu^p - \lambda^p}{(1-\lambda)(\mu^p - 1)(\mu - \lambda)} + \frac{L\epsilon_1}{(\mu^p - 1)(\mu - \lambda)} \left(\frac{\mu^p - 1}{\mu - 1} - \frac{1-\lambda^p}{1-\lambda} \right) \\
&= \frac{\epsilon_2}{1-\lambda} + L\epsilon_1 \frac{\mu^p - \lambda^p - (1-\lambda^p)}{(1-\lambda)(\mu^p - 1)(\mu - \lambda)} + \frac{L\epsilon_1(\mu^p - 1)}{(\mu^p - 1)(\mu - \lambda)(\mu - 1)} \\
&= \frac{\epsilon_2}{1-\lambda} + \frac{L\epsilon_1}{(1-\lambda)(\mu - \lambda)} + \frac{L\epsilon_1}{(\mu - \lambda)(\mu - 1)} \\
&= \frac{\epsilon_2}{1-\lambda} + \frac{L\epsilon_1}{(1-\lambda)(\mu - 1)} \qquad (3.6)
\end{aligned}
$$

Adding (3.5) and (3.6) completes the proof. □

From these relations, we see that ϵ_1, ϵ_2 small imply that the trajectory segment $\{(x_n, y_n), \ldots, (x_{n+p-1}, y_{n+p-1})\}$ is close to a period p orbit. Furthermore, for a reasonably smooth performance function F, the average of F over this piece of trajectory and the average of F on the nearby periodic orbit must be close to each other.

To be precise, if the performance function F has Lipschitz constant M, then

$$
\begin{aligned}
&\left| \frac{1}{p} \sum_{k=0}^{p-1} F(x_{n+k}, y_{n+k}) - \frac{1}{p} \sum_{k=0}^{p-1} F(x_k^*, y_k^*) \right| \\
&\qquad \leq \frac{1}{p} \sum_{k=0}^{p-1} |F(x_{n+k}, y_{n+k}) - F(x_k^*, y_k^*)| \\
&\qquad \leq \frac{M}{p} \sum_{k=0}^{p-1} \left(|x_{n+k} - x_k^*| + |y_{n+k} - y_k^*| \right)
\end{aligned}
$$

$$\leq \frac{M}{p}\left[\left(\frac{1}{\mu-1}+\frac{L}{(1-\lambda)(\mu-1)}\right)\epsilon_1+\left(\frac{\epsilon_2}{1-\lambda}\right)\right]$$
$$= \frac{M}{p}(C_1\epsilon_1+C_2\epsilon_2) \tag{3.7}$$

Thus for every n and p,

$$\frac{1}{p}\left[\sum_{k=0}^{p-1}F(x_{n+k},y_{n+k})-M(C_1\epsilon_1+C_2\epsilon_2)\right]\leq\frac{1}{p}\sum_{k=0}^{p-1}F(x_k^*,y_k^*)$$

That is, $S(n,p)$ defined by

$$S(n,p)=\frac{1}{p}\left[\sum_{k=0}^{p-1}F(x_{n+k},y_{n+k})-M(C_1\epsilon_1+C_2\epsilon_2)\right]$$

is a lower bound for the average of F over the periodic orbit starting at (x_0^*,y_0^*), and therefore is a lower bound on the optimal average. Recall that $\epsilon_1=|x_{n+p}-x_n|$ and $\epsilon_2=|y_{n+p}-y_n|$ are dependent on n and p. For a particular segment of a trajectory, we refer to $S(n,p)$ as its "score" and $M(C_1\epsilon_1+C_2\epsilon_2)/p$ as its "penalty". The values of n and p that yield the highest score, will generally have a low penalty value which means that the corresponding segment is close to a periodic orbit. We denote by S_- the largest lower bound on the optimal average we can obtain from a given trajectory of length N:

$$S_-=\max_{0\leq n<n+p\leq N}S(n,p). \tag{3.8}$$

If our initial condition generates a trajectory that is dense in a chaotic attractor and if there is an optimal periodic orbit on the attractor, then as the length N of the trajectory that we use increases to infinity, the trajectory will come arbitrarily close to the optimal orbit. It follows that the maximum score S_- will approach the optimal average.

3.3 Experimental Results

For a general map $h : \mathbb{R}^m \to \mathbb{R}^m$ and Lipschitz performance function $F : \mathbb{R}^m \to \mathbb{R}$ with Lipschitz constant M, our method proceeds as follows for a given choice of the penalty coefficient C in (3.1).

Step 1: *Generate a trajectory* $\{z_k = h^k(z)\}$ *of length* N.

Step 2: *For each value of* n *and* p, *calculate the score* $S(n, p)$ *given by* (3.1). In a chaotic attractor, every periodic orbit is unstable, so we don't expect the trajectory to stay near a periodic orbit for too long. In our numerical experiments we put a bound of 20 on the value of p, figuring that larger period orbits are both unlikely to be optimal and unlikely to be visited closely by trajectories of the lengths we considered.

Step 3: *Maximize* $S(n, p)$ *over* n *and* p *to obtain lower bound* S_- *for the optimal average.* Our method predicts that the optimal periodic orbit lies close to the trajectory segment $\{z_n, \ldots, z_{n+p-1}\}$ that optimizes the score. If the true optimal period is less than our bound for p, then as described above we expect S_- to converge to the true optimal average as N approaches infinity.

In the results below, in addition to S_- we also show the average S_* of F on the maximizing trajectory segment. We find that S_* is generally a closer estimate than S_- to the optimal average S_{24} obtained by brute force. The size of the penalty $S_* - S_-$ also plays a role as in deciding on an appropriate value of C when one cannot determine it analytically.

3.3.1 Kaplan-Yorke Map

Substituting $\mu = 2$, $\lambda = 0.4$ and $g(x) = \frac{1}{\pi}\sin[2\pi(x-\omega)]$ into (3.2), we have the Kaplan-Yorke Map

$$x_{n+1} = 2x_n \pmod 1; \tag{3.9a}$$

$$y_{n+1} = 0.4y_n + \frac{1}{\pi}\sin(2\pi x_n), \tag{3.9b}$$

whose chaotic attractor is shown in Figure 3.1.

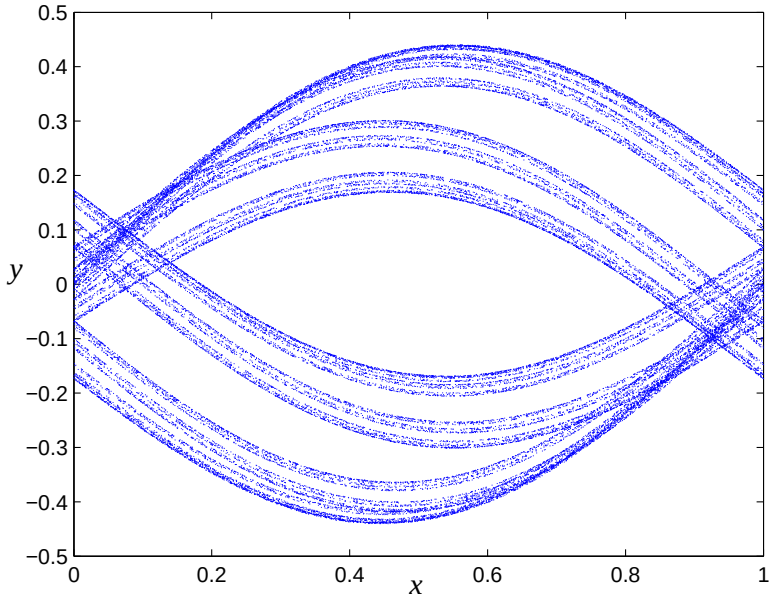

Figure 3.1: The Kaplan-Yorke Attractor. This figure was generated by iterating the map (3.9) 50 times starting at (0.1, 0.1) and plotting the next 40,000 iterations.

Recall for a given n and p we set $\epsilon_1 = |x_{n+p} - x_n|$ and $\epsilon_2 = |y_{n+p} - y_n|$. Taking $F_\omega(x) = \cos[2\pi(x + y - \omega)]$ as our performance function, and using the norm

$|(x,y)| = |x| + |y|$ we have $M = 2\pi$ and $L = 2$ so (3.7) becomes

$$\left| \frac{1}{p} \sum_{k=0}^{p-1} F(x_{n+k}, y_{n+k}) - \frac{1}{p} \sum_{k=0}^{p-1} F(x_k^*, y_k^*) \right| \leq \frac{2\pi}{p} \left[\left(1 + \frac{2}{1-0.4} \right) \epsilon_1 + \frac{\epsilon_2}{1-0.4} \right]$$

and the score is defined to be

$$S(n,p) = \frac{1}{p} \left[\sum_{k=0}^{p-1} F(x_{n+k}, y_{n+k}) - 2\pi \left(C_1 \epsilon_1 + C_2 \epsilon_2 \right) \right], \tag{3.10}$$

where $C_1 = \frac{13}{3}$ and $C_2 = \frac{5}{3}$. Figure 3.2 shows the optimal average and period obtained by brute force as a function of the parameter ω. Since the unstable part of the Kaplan-Yorke Map is the doubling map (3.9a), it is not surprising that the period verses parameter plot looks similar to that obtained from the doubling map with performance function $F_\omega(x) = \cos[2\pi(x - \omega)]$ (Fig. 2.1).

Over the next series of figures we show results for different trajectory lengths N, different choices of initial condition, and finally different values of the penalty coefficients C_1 and C_2. Each figure contains two graphs using 10,000 evenly spaced values of the parameter ω. Each of the top graphs shows the parameter versus optimal period for our method (the solid line) and for the brute force method (the dotted line). The lower graph of each figure shows the difference between our rigorous lower bound $S_- = \max S(n,p)$ and the brute force optimal average S_{24} together with $S_{\cdot} - S_{24}$ where $S_{\cdot}$ is the average of F_ω over the highest scoring segment found by our method.

The trajectories were generated by choosing x_0 and y_0 at random from $[0,1]$ and $[-0.5, 0.5]$ respectively, iterating (3.9) for 50 iterations so we can be sure that the trajectory is on the attractor, and then iterating N times more. For Figures 3.3 and 3.4 we use the same initial condition, but use 100,000 iterates for Fig. 3.3 and 500,000 for Fig. 3.4; we call this Trajectory 1.

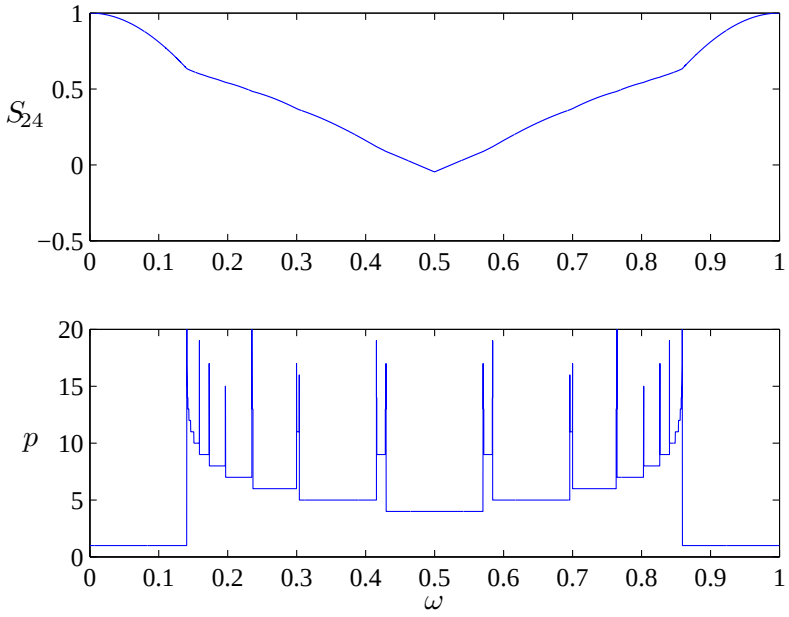

Figure 3.2: For the Kaplan-Yorke Map (3.9) with performance function $F_\omega(x, y) = \cos[2\pi(x + y - \omega)]$ we plot the maximum average S_{24} (upper graph) and optimal period p (lower graph) found by brute force (considering all periodic orbits up to period 24) for each of 10,000 evenly spaced values of ω.

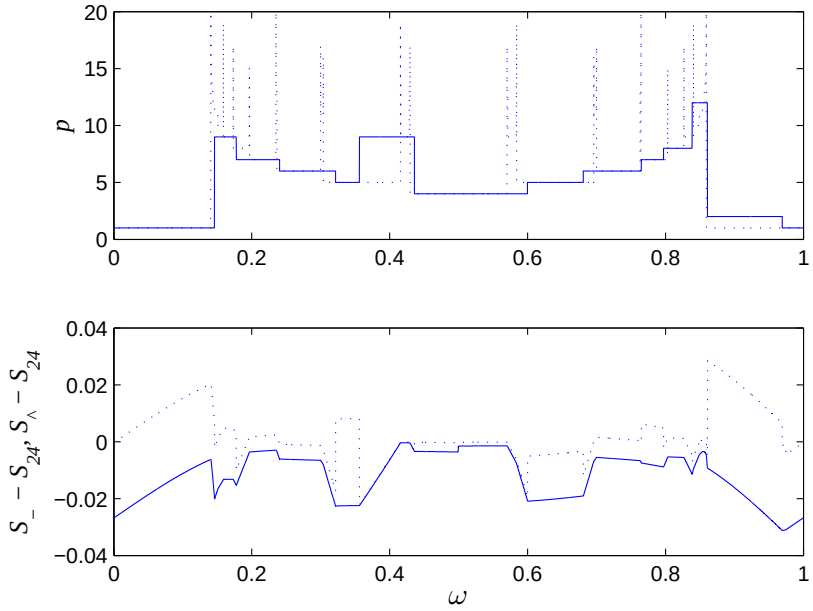

Figure 3.3: For the first $N = 100{,}000$ points of Trajectory 1 of the Kaplan-Yorke Map, and the performance function $F_\omega(x) = \cos[2\pi(x+y-\omega)]$, for 10,000 evenly spaced values of the parameter ω, we plot on the top graph the optimal period obtained from our method (solid line) and brute force (dotted line) while on the bottom graph we plot the differences between the results of our method and the brute force average S_{24}. The lower bound difference $S_- - S_{24}$ is the solid in the bottom graph, while the approximate average difference $S_{\wedge} - S_{24}$ is the dotted line.

Notice the different scales on the lower graphs of these figures. Like our one dimensional method, this method usually agrees the brute force optimal period when this period is low. However, there are more discrepancies, and generally we fail to find periods over 10. For this initial condition, extending the trajectory length from 100,000 to 500,000 increases the proportion of ω values at which our

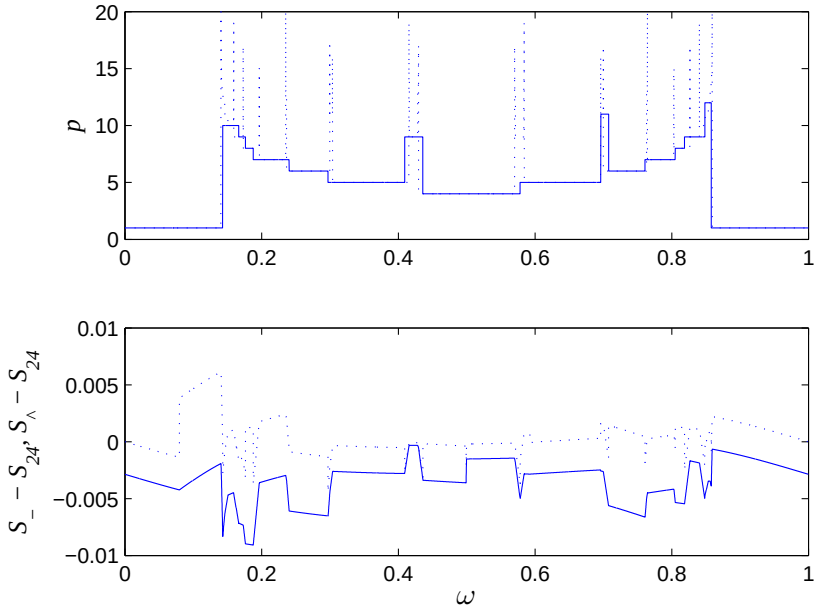

Figure 3.4: Optimal period and differences as in Fig. 3.3, for Trajectory 1, but now with length $N = 500,000$.

method and brute force method agree from 70% to 89%. The first number is a bit skewed due to the interval around $\omega = 0.9$ in Fig. 3.3, where our method finds a length two piece of the trajectory to be optimal. Those two points are very close (within 0.0001) to the fixed point rather than the period two orbit. In cases like this, our method locates the same periodic orbit as brute force, but the highest scoring segment of the trajectory follows the orbit for twice the period.

Of course all the results discussed above depend on the particular trajectory. In Fig. 3.5 we used a different initial condition to generate Trajectory 2 of length $N = 500,000$. In this case, the period we find agrees with the brute force period for 87% of the parameter values.

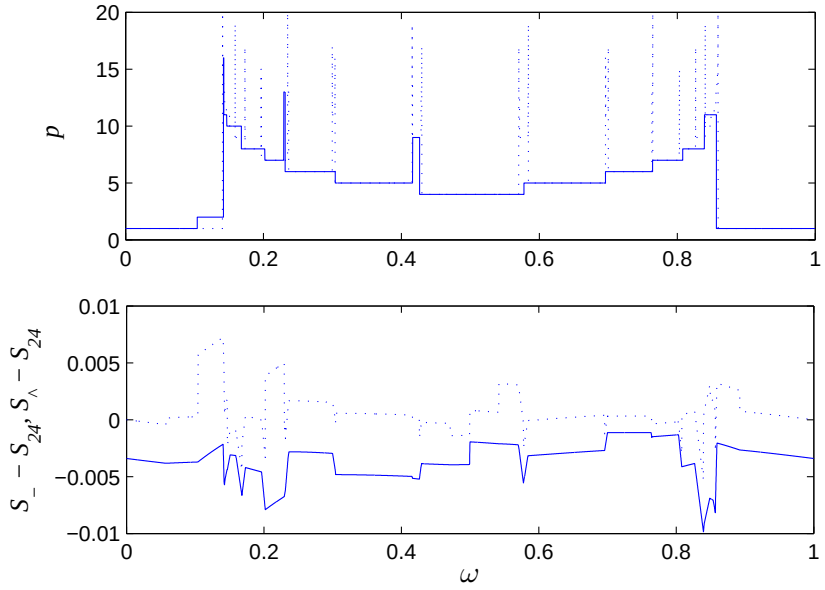

Figure 3.5: Optimal period and differences as in Fig. 3.3 using Trajectory 2 with $N = 500,000$. The results are qualitatively similar to those in Figure 3.4 for Trajectory 1, but differ significantly at some values of ω.

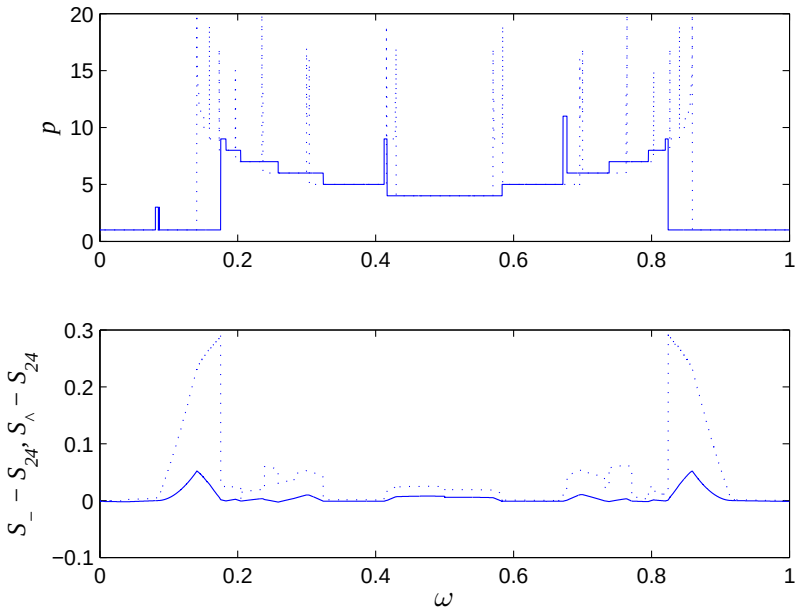

Figure 3.6: Optimal period and differences as in Fig. 3.3, using Trajectory 1 with penalty coefficients $C_1 = 13/6$ and $C_2 = 5/6$ in (3.10). These are half the values used in Fig. 3.4. Notice that the vertical scale on the bottom graph is quite different than in Fig. 3.4

.

Next, we vary the penalty in order to observe what happens when the penalty is either higher than it needs to be or too low to produce a rigorous bound. Our purpose is to help guide the choice of the penalty in cases when one cannot determine a rigorous value.

In Figure 3.6 we reduce the penalty coefficients C_1 and C_2 from their rigorous values by a factor of 2. In the lower graph, we see that S_- is indeed no longer a lower bound on S_{24}. For values of ω near 0.15 and 0.85, the maximum score occurs on a trajectory segment with a relatively large penalty; the penalty is the

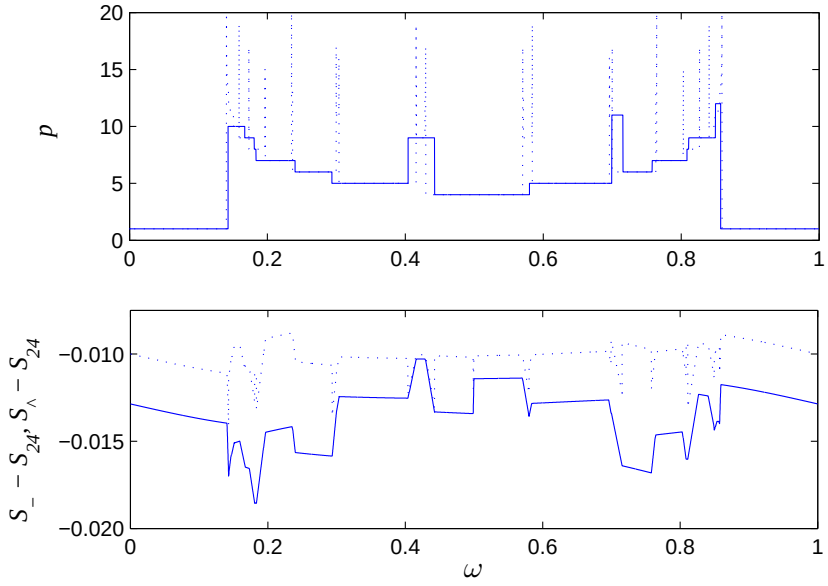

Figure 3.7: Optimal period and differences as in Fig. 3.3, using Trajectory 1 with penalty coefficients $C_1 = 26/3$ and $C_2 = 10/3$ in (3.10). These are twice the values used in Fig. 3.4.

difference $S_\wedge - S_-$ between the two curves. This means that the highest scoring segment is not even close to being periodic. This is an observation one could make without knowing S_{24}, and one should take such an occurrence to indicate that the penalty coefficients are too small.

On the other hand, when we double the penalty coefficients in Fig. 3.7, we don't see as much difference from Figure 3.4. For most values of ω, the value of $S_\wedge$ is the same, indicating that the same trajectory segment maximizes the score. Of course, the lower bound S_- is better when the penalty is smaller.

3.3.2 A Non-hyperbolic Case

Next we consider the Hénon map:

$$x_{n+1} = a + by_n - x_n^2, \tag{3.11}$$

$$y_{n+1} = x_n.$$

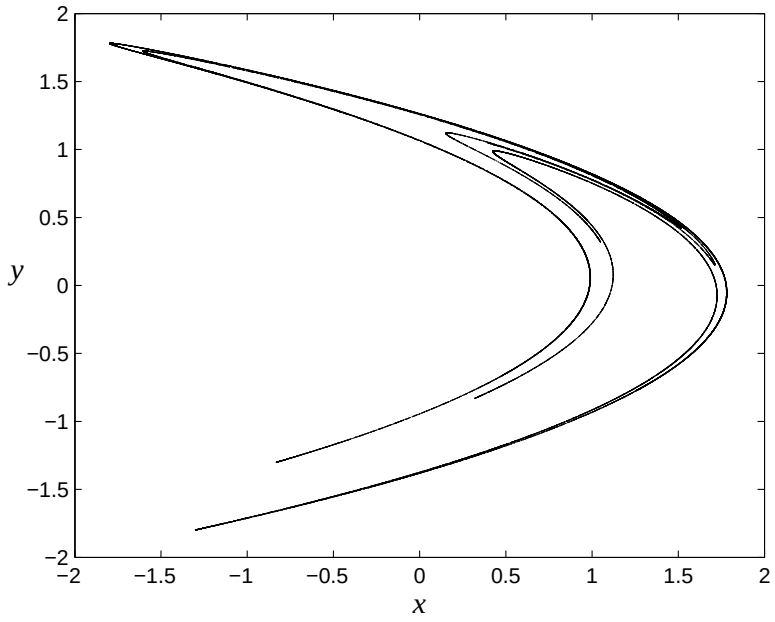

Figure 3.8: The Hénon attractor with parameter values $a = 1.4, b = 0.3$. This figure was generated by iterating the map (3.11) 50 times starting at (0.1,0.1) and plotting the next 40,000 iterates.

For $a = 1.4$ and $b = 0.3$ this map appears numerically to produce a non-hyperbolic chaotic attractor, shown in Fig 3.8. Though we cannot determine in this case a score function that gives a rigorous lower bound on the optimal average, we can compare the results we get for different penalty coefficients to a brute force optimal average using the algorithm of [3] to find the periodic orbits.

For performance function $F_\omega(x) = \cos[2\pi(\frac{x+y+2}{4} - \omega)]$, Fig. 3.9 shows the optimal average S_{24} and period p obtained by brute force as a function of parameter ω.

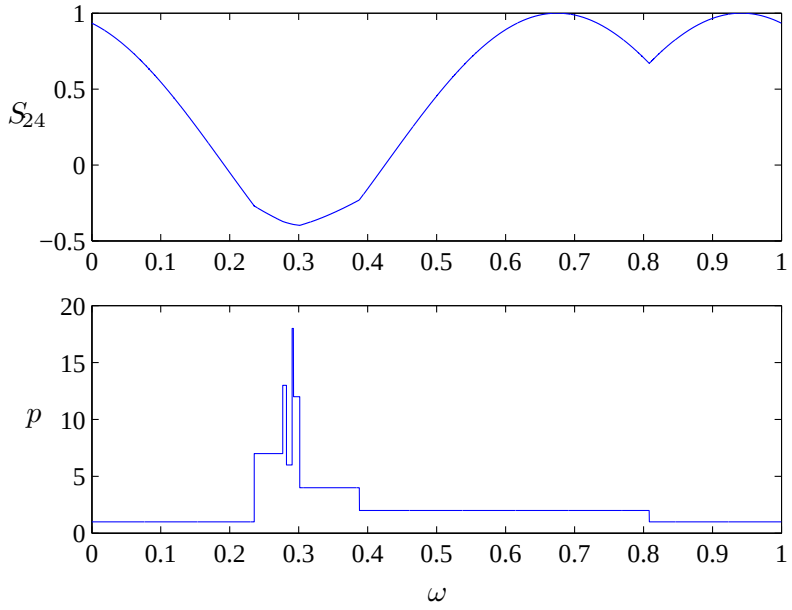

Figure 3.9: For the Hénon Map (3.11) with performance function $F_\omega(x, y) = \cos[2\pi(\frac{x+y+2}{4} - \omega)]$ we plot the maximum average S_{24} (upper graph) and optimal period p (lower graph) found by brute force (considering all periodic orbits up to period 24) for each of 10,000 evenly spaced values of ω.

In Section 3.3.1, we used different penalty coefficients C_1 and C_2 to multiply $\epsilon_1 = |x_n - x_{n+p}|$ and $\epsilon_2 = |y_n - y_{n+p}|$. This was because in the Kaplan-Yorke map, the y direction is the contracting direction at each point. For the Hénon map, the expanding and contracting directions are not aligned with coordinate axes, so we use a single penalty coefficient C_H. With $F_\omega(x) = \cos[2\pi(\frac{x+y+2}{4} - \omega)]$

as our performance function, we have $M = \pi/2$ and our score function is then

$$S(n,p) = \frac{1}{p}\left[\sum_{k=0}^{p-1} F_\omega(x_{n+k}, y_{n+k}) - \frac{\pi}{2} C_H(|x_n - x_{n+p}| + |y_n - y_{n+p}|)\right].$$

We could of course use the Euclidean distance between (x_n, y_n) and (x_{n+p}, y_{n+p}), but this slows down the computation while not improving the results.

The choice of the constant C_H is not obvious, but we can use what we learned from varying the penalty constant in the previous section (Figs. 3.4, 3.6, 3.7). Toward this end, we try several values of C_H, reducing it until we see large values of the penalty $S_\wedge - S_-$ for the best scoring trajectory segment. This indicates that we have reduced C_H too far, and we return to the previous value.

We want to intelligently choose a starting value of C_H. Recall that for the hyperbolic system (3.2), we derived the penalty coefficients

$$C_1 = [1 + L/(1-\lambda)]/(1-\mu) \quad \text{and} \quad C_2 = 1/(1-\lambda) \tag{3.12}$$

where μ was the expansion rate, λ was the contraction rate, and the constant L is related (inversely) to the minimum angle between the expanding and contracting directions. Although the Hénon attractor doesn't have well-defined contracting and expanding directions, we can use for μ and λ the computed Lyapunov numbers of (3.11). From the Dynamics program [15], we obtain Lyapunov numbers 1.5 and 0.2. A reasonable value for L is more problematic. Keeping in mind that the periodic orbits within a chaotic attractor do generally have expanding and contracting directions, and that among the low period orbits that are most likely to be optimal the angle between these directions is not likely to get too close to zero, we suggest that a moderate value of L may be reasonable in practice. Substituting $L = 1$, $\mu = 1.5$ and $\lambda = 0.2$ into (3.12) we have $C_1 = 4.25$ and $C_2 = 1.25$. Thus we start in Fig. 3.10 with $C_H = 4$.

As in the previous section, we generate a trajectory of length $N = 500,000$ and maximize $S(n,p)$ for 10,000 equally spaced values of the parameter ω. Figures 3.10 to 3.12 show the difference between $S_- = \max S(n,p)$ and the brute force optimal average S_{24} together with $S_\wedge - S_{24}$, where $S_\wedge$ is the average of F_ω over the highest scoring segment found by our method. While S_- is no longer a rigorous lower bound on the optimal average, we find that for suitable values of C_H that it remains below S_{24} (which is itself a lower bound on the optimal average).

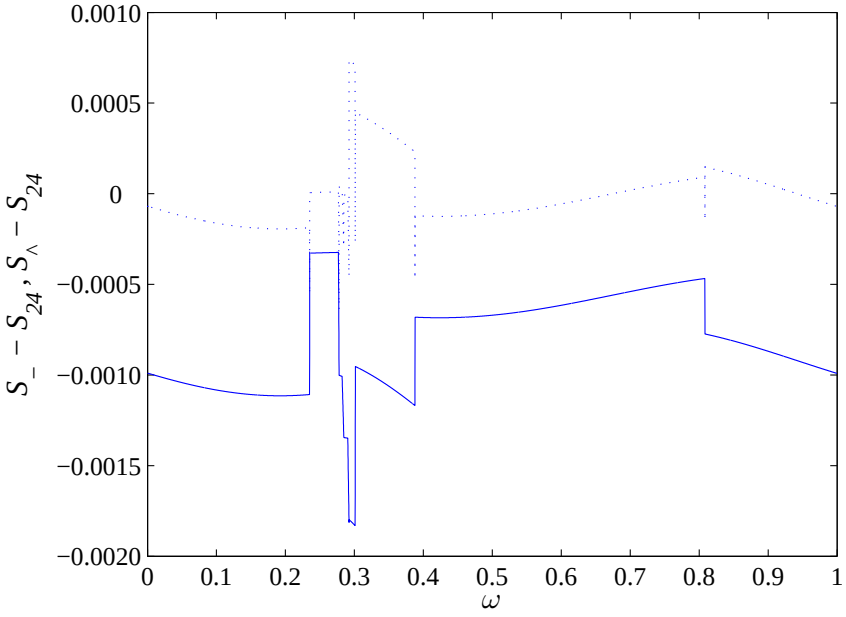

Figure 3.10: Using penalty coefficient $C_H = 4.0$, a trajectory length $N = 500,000$ for the Hénon Map (3.11), and the performance function $F_\omega(x) = \cos[2\pi(\frac{x+y+2}{4} - \omega)]$, for 10,000 evenly spaced values of the parameter ω, we plot the differences of maximum score S_- and estimated maximum average $S_\wedge$ with the brute force average S_{24}. The difference $S_- - S_{24}$ is the solid line, while $S_\wedge - S_{24}$ is the dotted line.

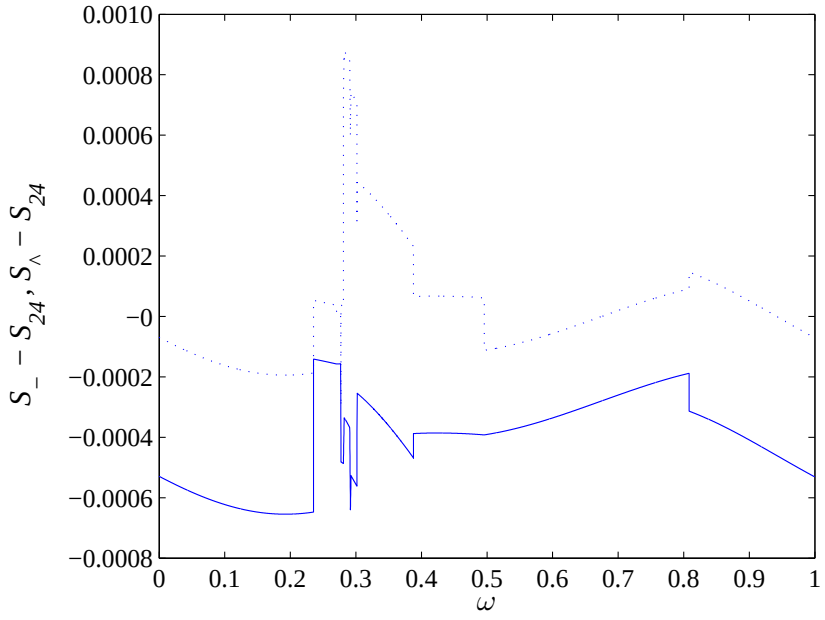

Figure 3.11: The same quantities as in Figure 3.10, but now with penalty coefficient $C_H = 2.0$.

In Fig. 3.10, we don't see regions of parameter space for which the penalty $S\hat{} - S_-$ is high. In Fig. 3.11, we reduce the value of C_H from 4 to 2. Comparing the two figures, we see that S_- uniformly gets closer to S_{24} in Fig. 3.11, but the penalty has begun to increase slightly around $\omega = 0.3$. Reducing C_H to 1 in Fig. 3.12, we see a large interval of parameter values for which the penalty $S\hat{} - S_-$ is quite large, indicating that the optimal segment of trajectory found by our method is not close to being periodic. Furthermore, S_- is no longer a lower bound on the brute force maximum average. Thus we settle on the value $C_H = 2$ for the penalty coefficient.

In Fig. 3.13, we show the length p of the trajectory segment that maximizes the score $S(n, p)$, compared with the brute force optimal period, as a function

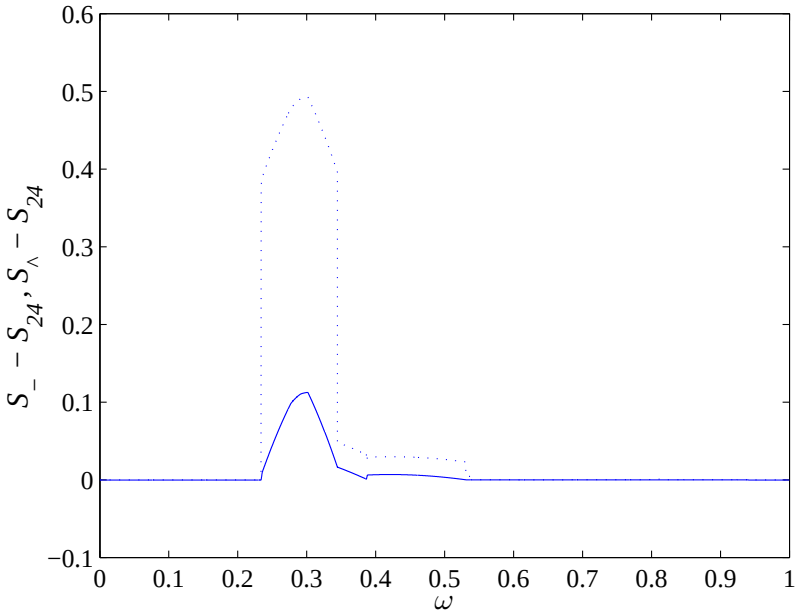

Figure 3.12: The same quantities as in Figure 3.10, but now with penalty coefficient of $C_H = 1$. The large penalty for an interval of values around $\omega = 0.3$ indicates that this value of C_H is too small.

of ω. We see significant improvement in the agreement between the methods in going from the first 100,000 points of our trajectory to 500,000 points. The remaining discrepancies are almost entirely at places where the highest scoring trajectory segment has length twice the brute force optimal period. For these parameter values, we checked that the trajectory segment stays close to the brute force optimal orbit for two period. (This occurs more frequently than for the Kaplan-Yorke map because the Hénon map is not orientation preserving. The linearized map at the fixed point, for example, has a negative eigenvalue, so that a trajectory segment of length 2 near the fixed point can have a smaller penalty than any length 1 segment.) This example suggests that even in a non-hyperbolic

case, with a well chosen penalty coefficient, our method typically is able to find a trajectory segment in the vicinity of the optimal orbit with a sufficiently long trajectory. Also, if the optimal orbit has reasonably low period, the trajectory can be of moderate length.

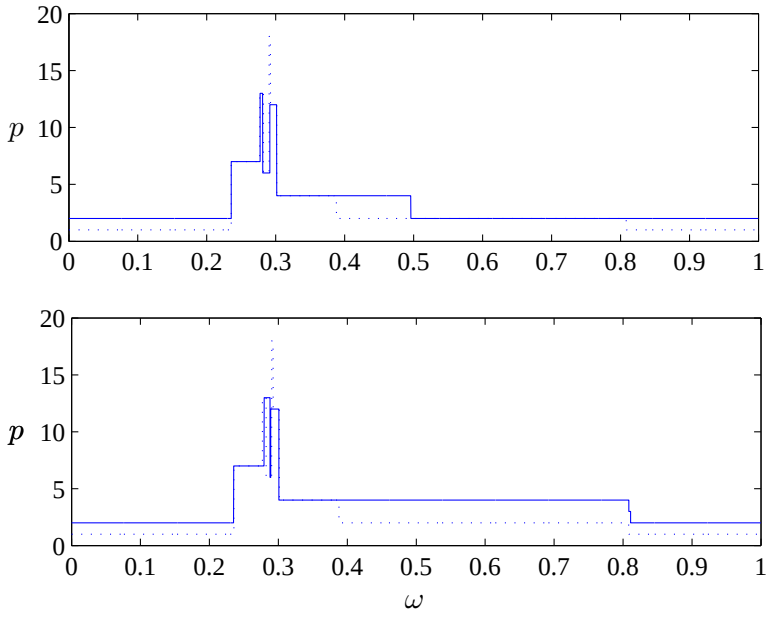

Figure 3.13: Comparison of the value of p that maximizes the score (solid curve) with the optimal period found by brute force (dotted curve). For the top graph, we maximized the score over the entire trajectory of length $N = 500,000$, while for the bottom graph we used only the first $N = 100,000$ points. For both graphs we used $C_H = 2$, and the trajectory and other parameters as in Fig 3.10.

3.4 Conclusion

We have described a method that indicates where on a chaotic attractor to look for an optimal periodic orbit, given a scalar "performance function" whose time average is to be maximized, and a trajectory on the attractor. The method is most practical for systems with lower dimensional attractors, where a trajectory of reasonable length can be expected to pass close to all the periodic orbits of the attractor with relatively low period.

For hyperbolic systems, our method also yields a rigorous lower bound on the optimal average. For non-hyperbolic systems, one must tune a parameter C, the "penalty coefficient", of the method. By example we have indicated how to choose this parameter. Our analysis of the hyperbolic case suggests that in general C should be comparable in size to $(\mu - 1)^{-1}(1 - \lambda)^{-1}$, where μ and λ are the expanding and contracting Lyapunov numbers of the attractor that are closest to one. Values of C that are too small can produce unrealistic results identifying a segment of the trajectory that is not even close to being periodic. We suggest adjusting C just high enough to avoid such occurrences, not only for the performance function of interest, but for a family of similar performance functions. With this approach we found good agreement of our method with brute force optimization over a large number of periodic orbits.

BIBLIOGRAPHY

[1] J.C. Alexander, I. Kan, J.A. Yorke, and Z-P. You, *Riddled basins*, Intl. Journal of Bifurcation and Chaos **2** (1992), no. 795.

[2] P. Ashwin, J. Buescu, and I. Stewart, *Bubbling of attractors and synchronisation of chaotic oscillators*, Phys. Lett. A **193** (1994), no. 126.

[3] O. Biham and W. Wenzel, *Characterization of unstable periodic orbits in chaotic attractors and repellers*, Phys. Rev. Lett. **63** (1989), 819–822.

[4] T. Bousch, *Le poisson n'a pas d'arêtes*, CNRS URA **1169** (1998).

[5] R. Bowen and D. Ruelle, *The ergodic theory of Axiom-A flows*, Inv. Math **29** (1975), 181–202.

[6] G. Contreras, A.O. Lopes, and P. Thieullen, *Lyapunov minimizing measures for expanding maps of the circle*, Ergod. Th. and Dynam. Sys. **21** (2001), 1–31.

[7] C. Grebogi, E. Ott, T. Shinbrot, and J.A. Yorke, *Using small perturbations to control chaos*, Nature **363** (1993), 411–417.

[8] B. Hasselbratt and A. Katok, *Introduction to modern theory of dynamical systems*, Cambridge University Press, 1995.

[9] B. Hunt and E. Ott, *Optimal periodic orbits of chaotic systems occur at low period*, Phys. Rev. E **54** (1996).

[10] B. Hunt and G. Yuan, *Optimal orbits of hyperbolic systems*, Nonlinearity **12** (1999), 1207–1224.

[11] O. Jenkinson, *Frequency-locking on the boundary of the barycentre set*, Experimental Mathematics **9** (2000).

[12] A. Lasota and J. A. Yorke, *On the existence of invariant measures for piecewise monotonic transformations*, Trans. Amer. Math. Soc. **186** (1973), 481–488.

[13] A.O. Lopes and P. Thieullen, *Sub-actions for anosov diffeomorphisms*, Asterisque: Geometric Methods in Dynamics (II) **297** (2003), 135–146.

[14] R. Mañé, *Generic properties and problems of minimizing measures of lagrangian systems*, Nonlinearity **9** (1996), 273–310.

[15] H. Nusse and J. Yorke, *Dynamics: Numerical exploations*, Springer-Verlag, 1997.

[16] M. Pollicott and R. Sharp, *Livsic theorems, maximizing measures and the stable norm*, Dynamical Systems: An International Journal **19** (2004), 75–88.

[17] Ya. G. Sinai, *Gibbs measures in ergodic theory*, Russ. Math. Surveys **27** (1972), no. 4, 21–70.